Nuclear Physics B348 (1991) 591–618
North-Holland

THE SCALING REGION OF THE TRICRITICAL ISING MODEL IN TWO DIMENSIONS

Michael LÄSSIG, Giuseppe MUSSARDO* and John L. CARDY

Department of Physics, University of California, Santa Barbara, CA 93106, USA

Received 31 May 1990

We study the scaling region spanned by all four relevant perturbations of the tricritical Ising model in two dimensions. We analyze the spectrum of the (1 + 1)-dimensional off-critical hamiltonian on a truncated Hilbert space, a method recently proposed by Yurov and Al. Zamolodchikov. In the phase coexistence regions the massive excitations are kink states. On the temperature-driven two-phase coexistence line, they form bound states, which we analyze for periodic as well as for twisted boundary conditions. We find a new asymmetric two-phase region driven by the subleading magnetic field. There are some indications of massless states along the crossover line to the Ising model. The effects of off-critical integrability on the spectra are also observed and discussed.

1. Introduction

Next to the Ising model, the tricritical Ising model is the second simplest unitary conformal field theory in two dimensions [1,2]. Its central charge is $c = 7/10$, and there are four relevant scaling fields. It represents the universality class of the Landau–Ginzburg Φ^6-theory at its tricritical point [3]. Thus it describes tricritical phenomena in a variety of microscopic models, among them the Ising model with annealed vacancies [4,5].

The tricritical Ising model is a theorist's ideal playground. It is particularly interesting due to its various infinite-dimensional symmetries: conformal symmetry, super-conformal symmetry (the tricritical Ising model is the first member of the series of super-conformal minimal models [6]), and the symmetries based on the algebras su(2) and e_7 (related to the coset constructions $su(2)_2 \otimes su(2)_1/su(2)_3$ and $(e_7)_1 \otimes (e_7)_1/(e_7)_2$ [7,8]).

A generic perturbation of the critical model will destroy all of these symmetries. But for some specific perturbations, a subset of them survives away from criticality. In these cases, the perturbed theory remains integrable, and it has an infinite number of conserved currents J_s with spin s [9]. The set $\{s\}$ is given by the

* INFN Fellow, Sez. di Trieste, Italy.

particular integrable deformation of the critical theory. The integrability of the off-critical theory has striking consequences for the corresponding $(1+1)$-dimensional quantum field theory: it allows for the exact computation of the particle masses and the S-matrix.

The renormalization group scenario of the perturbed tricritical Ising model is severely constrained by Zamolodchikov's c-theorem [10]. This theorem asserts that there exists a function c on the space of two-dimensional unitary field theories that is monotonically decreasing along renormalization group trajectories and is stationary only at fixed points, where it equals the central charge c of the corresponding conformal field theory. Hence any unitary deformation of the tricritical Ising model is described in the infrared limit by either the massive fixed point ($c = 0$) or the Ising fixed point ($c = \frac{1}{2}$).

In the present paper, we present a detailed investigation of the scaling region around the tricritical Ising fixed point. The method we use was recently developed by Yurov and Al. Zamolodchikov [11]. It can be stated in the language of quantum field theory on the strip. The conformal theory defines the basis of the Hilbert space and the unperturbed hamiltonian H_0, while the perturbation gives rise to an interaction term V. The matrix elements of H_0 and V between the conformal states are given in terms of the anomalous dimensions and the structure constants of the conformal theory. One can then numerically diagonalize the off-critical hamiltonian on a suitably truncated Hilbert space and study the spectrum as a function of the strip width R; the behavior for large R contains the information on the infrared theory.

This method proves to be well suited for the study of the tricritical Ising model; being essentially nonperturbative, it avoids some difficulties that the ε-expansion incurs in this case (see subsect. 4.2). The numerical data show the existence of various phase coexistence regions, among them one generated by the subleading magnetic field. This is remarkable since this perturbation explicitly breaks the spin-reversal symmetry of the conformal theory.

The mass spectra agree well with the theoretical predictions in the integrable cases [9, 12–14]. We discuss in detail the interpretation of the massive particles as kink states in the phase coexistence regions. Imposing antiperiodic boundary conditions makes it possible to see also the fermionic sector of the theory. It is more difficult, however, to observe with this method the massless states along the crossover line to the Ising model.

This paper is organized as follows. In sect. 2, we discuss generalities of finite-size scaling on the strip and the truncation method. In sect. 3 we collect the necessary information about the theory at the conformal point: the operator content of the tricritical Ising model, its structure constants, and the partition function with periodic or antiperiodic boundary conditions. In sect. 4 we analyze the magnetic perturbations and in sect. 5 the energy perturbations of the tricritical Ising model. Sect. 6 contains our conclusions.

2. Finite-size scaling on the strip and the truncation method

Consider a euclidean conformal field theory in the plane which is perturbed by a relevant scaling field with angular momentum $\Delta - \bar{\Delta} = 0$ and scaling dimension $\Delta + \bar{\Delta} = x$. The euclidean action is

$$\mathscr{A}_\lambda = \mathscr{A}_0 + \lambda \int \phi_{\Delta,\Delta}(z, \bar{z})\, \mathrm{d}^2 z\,, \tag{2.1}$$

with a coupling constant λ having dimension $y = 2 - x > 0$. The perturbation expansion of the correlation functions suffers from infrared divergences and, for $x > 1$, from ultraviolet divergences as well. Via the logarithmic mapping

$$\omega \equiv u + iv = \frac{R}{2\pi} \ln z\,, \tag{2.2}$$

the action (2.1) defines a euclidean quantum field theory on a strip of width R, with the hamiltonian (the logarithm of the transfer matrix)

$$H_\lambda = H_0 + \lambda V. \tag{2.3}$$

The "unperturbed" part of the hamiltonian can be expressed in terms of the Virasoro generators $L_0, \bar{L}_0$, and the central charge c [15],

$$H_0 = \frac{2\pi}{R}\left(L_0 + \bar{L}_0 - \frac{c}{12}\right), \tag{2.4}$$

while the interaction term V is given by

$$V = \int_0^R \phi_{\Delta,\Delta}(\omega, \bar{\omega})\, \mathrm{d}v\,. \tag{2.5}$$

Since $\phi_{\Delta,\Delta}$ is rotation scalar in the plane, both H_0 and V commute with the momentum operator on the strip,

$$K = \frac{2\pi}{R}(L_0 - \bar{L}_0)\,. \tag{2.6}$$

Now one chooses a Hilbert space basis of eigenstates of H_0. These "conformal states" are labelled by their energy, their momentum, and additional quantum numbers. The matrix elements of V between them,

$$\langle \phi_j | V | \phi_i \rangle = \frac{R}{2\pi} \langle \phi_j | \phi_{\Delta,\Delta}(0,0) | \phi_i \rangle \delta_{K_j, K_i}\,, \tag{2.7}$$

can be expressed in terms of conformal three-point functions in the plane. By virtue of the infinite-dimensional conformal symmetry, these in turn can be computed from a finite number of (dimensionless) primary structure constants which characterize the dynamics of the theory. The technicalities of this calculation are deferred to appendix A.

After a suitable truncation of the Hilbert space, the problem of finding the off-critical spectrum is thus reduced to numerical matrix diagonalization. Yurov and Al. Zamolodchikov [11] introduced this method and applied it to the integrable off-critical Yang–Lee model [17]. They showed that a space truncated to a moderate number of states gives a spectrum which is surprisingly similar to that of the infinite Hilbert space in the massive regime.

The energy levels $E_i (i = 0, 1, 2, \ldots)$ on a strip of width R are expected to have the scaling form

$$E_i(R, \lambda) = \frac{2\pi}{R} f_i\left(\frac{R}{\xi}\right), \tag{2.8}$$

where $\xi(\lambda)$ is the correlation length of the theory, defined as the inverse of the lowest mass gap m_1. If the massive system is integrable, $\xi(\lambda)$ can be computed from the thermodynamic Bethe ansatz [16]. In the present context, we are interested only in dimensionless mass ratios. The ultraviolet asymptotic spectrum is that of H_0,

$$E_i \simeq \frac{2\pi}{R}\left(x_i - \frac{c}{12}\right) \qquad (R \ll \xi), \tag{2.9}$$

where $x_i = \Delta_i + \bar{\Delta}_i$ (Δ_i and $\bar{\Delta}_i$ are eigenvalues of L_0 and $\bar{L}_0$, respectively). In the infrared regime, the scaling functions f_i become

$$f_i \simeq \frac{1}{2\pi}\left[\epsilon_0\left(\frac{R}{\xi}\right)^2 + \frac{m_i}{m_1}\frac{R}{\xi}\right] \qquad (R \gg \xi), \tag{2.10}$$

so that

$$E_i(R) \simeq \frac{\epsilon_0}{\xi^2} R + m_i \qquad (R \gg \xi), \tag{2.11}$$

where m_i is the mass gap of the ith level. The dimensionless constant ϵ_0 can be interpreted as the universal contribution to the vacuum bulk energy density (energies measured in units of m_1 and lengths in units of $\xi = 1/m_1$). For an integrable massive system, it can be computed from the thermodynamic Bethe ansatz [16] as well.

Which levels are present in the spectrum depends on the boundary conditions (see the detailed discussion in subsect. 4.3). In a disordered phase, the lowest line

$E_0 = \epsilon_0 R/\xi^2$ is always present; in an ordered phase, this depends on the boundary conditions.

The scaling form (2.8) of the energies is somewhat modified by the truncation of the Hilbert space. In the full Hilbert space, the matrix elements of H_0 are unbounded from above; hence for any finite λ, the eigenstates of H_λ are nontrivial combinations of the eigenstates of H_0 and those of V. The truncation imposes an upper bound to the matrix elements of H_0. This introduces an additional scale ρ and leads to the scaling form for the energies

$$E_i^{\mathrm{tr}}(R) = \frac{2\pi}{R} f_i^{\mathrm{tr}}\left(\frac{R}{\xi}, \frac{R}{\rho}\right). \tag{2.12}$$

For large λ (or equivalently, for $R \gg \rho$), the matrix elements of H_0 become negligible against those of λV; the asymptotic eigenstates are those of V. In this unphysical regime the energies scale like

$$E_i^{\mathrm{tr}} \sim \lambda R^{y-1} \qquad (R \gg \rho). \tag{2.13}$$

The correlation length ξ characterizes the crossover from the ultraviolet regime to the infrared regime, while the scale ρ governs the onset of truncation effects. To extract reliable information about the infrared region, a sufficient number of states has to be included in order that $\rho \gg \xi$. In this case, the R-dependence of the levels shows the three distinct scaling regimes (2.9), (2.11) and (2.13), separated by two crossover regions at $R \sim \xi$ and $R \sim \rho$.

An interesting situation occurs when the deformation of the conformal theory happens to be integrable. In this case, there exists a set of conserved currents (T_{s+1}, Θ_{s-1}) satisfying

$$\partial_{\bar{z}} T_{s+1} = \partial_z \Theta_{s-1}. \tag{2.14}$$

The set $\{s\}$ is given by the particular integrable deformation. By transforming onto the strip and integrating over a surface of equal time, we obtain integrals of motion

$$\mathcal{Q}_s = \frac{1}{2\pi} \int_0^R \left(T_{s+1}^{\mathrm{strip}} + \Theta_{s-1}^{\mathrm{strip}}\right)_{uu}(w)\, \mathrm{d}v. \tag{2.15}$$

The Hilbert space and the dynamics decompose into sectors according to different values of the charges (2.15). This may be observed in the R-dependence of the spectrum [11]: two levels from different sectors of the Hilbert space may cross each other, while generic lines (in the absence of any symmetry) do not cross. For the integrable deformations of the tricritical Ising model, we find level crossings which we attribute to the higher conserved charges; this is discussed in subsect. 4.2.

TABLE 1
Kac table of the tricritical Ising model

$\frac{3}{2}$	$\frac{7}{16}$	0
$\frac{6}{10}$	$\frac{3}{80}$	$\frac{1}{10}$
$\frac{1}{10}$	$\frac{3}{80}$	$\frac{6}{10}$
0	$\frac{7}{16}$	$\frac{3}{2}$

3. The tricritical Ising model

The tricritical Ising model is the second member $\mathcal{M}_4$ of the unitary series of minimal models $\mathcal{M}_m$ $(m = 3, 4, \ldots)$. It represents the universality class of the Landau–Ginzburg theory

$$\int \mathcal{D}\Phi \exp\left\{ - \int \left[(\nabla\Phi)^2 + \lambda_6 \Phi^6 + \lambda_4 \Phi^4 + \lambda_3 \Phi^3 + \lambda_2 \Phi^2 + \lambda_1 \Phi \right] \mathrm{d}^2 r \right\} \quad (3.1)$$

at its tricritical point $\lambda_1 = \lambda_2 = \lambda_3 = \lambda_4 = 0$. Its operator algebra has a basis of spinless scaling fields $\phi_{\Delta,\bar{\Delta}}$, labelled by the conformal dimensions $\Delta, \bar{\Delta}$. The six primary fields appearing in the Kac table (table 1) can be identified with normal-ordered composite Landau–Ginzburg fields [3]. According to their transformation properties under the $\mathbb{Z}_2$ spin-reversal transformation Q: $\Phi \to -\Phi$, we have:

(i) Four even fields: the identity $1 \equiv \phi_{0,0}$, the leading energy density $\varepsilon \equiv \phi_{\frac{1}{10},\frac{1}{10}} = :\Phi^2:$, the subleading energy density* $\varepsilon' \equiv \phi_{\frac{6}{10},\frac{6}{10}} = :\Phi^4:$, and the irrelevant field $\varepsilon'' \equiv \phi_{\frac{3}{2},\frac{3}{2}} = :\Phi^6:$. These fields form a subalgebra of the operator algebra. In this subalgebra, Kramers–Wannier duality acts as a second $\mathbb{Z}_2$ symmetry under which ε and ε'' are odd and ε' is even:

$$D^{-1}\varepsilon D = -\varepsilon, \qquad D^{-1}\varepsilon' D = \varepsilon'. \quad (3.2)$$

(ii) Two odd fields: the leading magnetization $\sigma = \phi_{\frac{3}{80},\frac{3}{80}} = \Phi$, and the subleading magnetization $\sigma' = \phi_{\frac{7}{16},\frac{7}{16}} = :\Phi^3:$.

The composite field $:\Phi^5:$ is redundant in the sense of the renormalization group and is not a primary field of the operator algebra.

In the supersymmetric formulation of the theory [6], the energy densities build up the superfield in the Neveu–Schwarz sector,

$$\mathcal{N}(z, \bar{z}, \theta, \bar{\theta}) = \varepsilon(z, \bar{z}) + \bar{\theta}\psi(z, \bar{z}) + \theta\bar{\psi}(z, \bar{z}) + \theta\bar{\theta}\varepsilon'(z, \bar{z}), \quad (3.3)$$

while the magnetic fields are representations in the Ramond sector.

* In the site-diluted Ising model, this field couples to the density of vacancies.

TABLE 2
Operator content of the tricritical Ising model with periodic boundary conditions

$\sigma = [\frac{3}{80}, \frac{3}{80}] = \Phi$	magnetization
$\varepsilon = [\frac{1}{10}, \frac{1}{10}] = :\Phi^2:$	energy
$\sigma' = [\frac{7}{16}, \frac{7}{16}] = :\Phi^3:$	sub-magnetization
$\varepsilon' = [\frac{6}{10}, \frac{6}{10}] = :\Phi^4:$	vacancy density
$\varepsilon'' = [\frac{3}{2}, \frac{3}{2}] = :\Phi^6:$	(irrelevant)

The operator content of the theory on the strip depends on the boundary conditions imposed [15]. For periodic boundary conditions, the partition function of the tricritical Ising model is given by the diagonal solution of the modular equations [24]

$$Z_{P,P} = \mathrm{Tr}\, e^{-H_0} = |\chi_0|^2 + |\chi_{\frac{3}{80}}|^2 + |\chi_{\frac{1}{10}}|^2 + |\chi_{\frac{7}{16}}|^2 + |\chi_{\frac{6}{10}}|^2 + |\chi_{\frac{3}{2}}|^2, \qquad (3.4)$$

leading to the operator content listed in table 2. The states have momenta that are integer multiples of $2\pi/R$, and we refer to them as bosonic states.

The partition function $Z_{A,P}$ with $\mathbb{Z}_2$-twisted boundary conditions in the space direction $\mathrm{Re}\,\omega$ may be obtained as follows [15]. First, insertion of the $\mathbb{Z}_2$-charge Q into (3.4) yields the partition function $Z_{P,A}$ with twisted boundary conditions in the time direction $\mathrm{Im}\,\omega$,

$$Z_{P,A} = \mathrm{Tr}\, Q e^{-H_0} = |\chi_0|^2 - |\chi_{\frac{3}{80}}|^2 + |\chi_{\frac{1}{10}}|^2 - |\chi_{\frac{7}{16}}|^2 + |\chi_{\frac{6}{10}}|^2 + |\chi_{\frac{3}{2}}|^2, \qquad (3.5)$$

which is related to $Z_{A,P}$ by the modular transformation S. Hence we obtain

$$Z_{A,P}(q) = |\chi_{\frac{3}{80}}|^2 + |\chi_{\frac{7}{16}}|^2 + [\chi_0^* \chi_{\frac{3}{2}} + \chi_{\frac{1}{10}}^* \chi_{\frac{6}{10}} + \mathrm{c.c.}], \qquad (3.6)$$

and from this expression we can read off which operators appear with twisted boundary conditions. The primary operators are (see table 3):

(i) The disorder operators

$$\mu = D^{-1}\sigma D = \tilde{\phi}_{\frac{3}{80},\frac{3}{80}}, \qquad \mu' = D^{-1}\sigma' D = \tilde{\phi}_{\frac{7}{16},\frac{7}{16}}. \qquad (3.7)$$

TABLE 3
Operator content of the tricritical Ising model with twisted boundary conditions

$\mu = [\frac{3}{80}, \frac{3}{80}]$	disorder field
$\mu' = [\frac{7}{16}, \frac{7}{16}]$	subleading disorder field
$\psi = [\frac{6}{10}, \frac{1}{10}]$	fermion
$\bar{\psi} = [\frac{1}{10}, \frac{6}{10}]$	anti-fermion
$G = [\frac{3}{2}, 0]$	susy generator
$\bar{G} = [0, \frac{3}{2}]$	susy generator

They are dual to the magnetic operators σ and σ' and have the same scaling dimensions. The elementary disorder field μ describes a string of reversed bonds on the lattice; the subleading disorder operator μ' is the composite field $:\mu\varepsilon:$. The states in this sector are bosonic. The appearance of the disorder fields may also be seen from the superconformal symmetry of the tricritical Ising model. The zero-modes of the supercurrent in the Ramond sector are given by

$$G_0^2 = L_0 - \frac{c}{24}, \qquad \overline{G}_0^2 = \overline{L}_0 - \frac{c}{24}; \tag{3.8}$$

they commute with the conformal hamiltonian (2.4). Since the tricritical Ising model does not have a primary operator with dimension $\Delta = c/24$, eq. (3.8) implies the existence of the two degenerate ground states $|\sigma\rangle$ and $|\mu\rangle = G_0\overline{G}_0|\sigma\rangle$ in the Ramond sector.

(ii) The fermion $\psi = \tilde{\phi}_{\frac{6}{10},\frac{1}{10}}$, the antifermion $\overline{\psi} = \tilde{\phi}_{\frac{1}{10},\frac{6}{10}}$, and the supersymmetry generators $G = \tilde{\phi}_{\frac{3}{2},0}$ and $\overline{G} = \tilde{\phi}_{0,\frac{3}{2}}$. Particles and antiparticles are related by duality:

$$\overline{\psi} = D^{-1}\psi D, \qquad \overline{G} = -D^{-1}GD. \tag{3.9}$$

In this sector, the momenta are half-integer multiples of $2\pi/R$.

The operator algebra (which is given for the bosonic sector in table 4 and for the fermionic sector in table 5) reflects the mentioned symmetries of the scaling fields. This structure leads to symmetries and selection rules for the off-critical theories as well. In the following, we discuss the deformations of the tricritical Ising model

TABLE 4
Fusion rules and structure constants for the scalar fields of the tricritical Ising model

even * even	
$\varepsilon * \varepsilon = [1] + c_1[\varepsilon']$	$c_1 = \frac{2}{3}\sqrt{\frac{\Gamma(\frac{4}{5})\Gamma^3(\frac{2}{5})}{\Gamma(\frac{1}{5})\Gamma^3(\frac{3}{5})}}$
$\varepsilon' * \varepsilon' = [1] + c_2[\varepsilon']$	$c_2 = c_1$
$\varepsilon * \varepsilon' = c_1[\varepsilon] + c_3[\varepsilon'']$	$c_3 = \frac{3}{7}$
$\varepsilon'' * \varepsilon'' = [1]$	$c_4 = \frac{1}{2}$
even * odd	$c_5 = \frac{3}{2}c_1$
$\varepsilon * \sigma' = c_4[\sigma]$	$c_6 = \frac{3}{4}$
$\varepsilon * \sigma = c_4[\sigma'] + c_5[\sigma]$	$c_7 = \frac{1}{4}c_1$
$\varepsilon' * \sigma' = c_6[\sigma]$	$c_8 = \frac{7}{8}c_1$
$\varepsilon' * \sigma = c_6[\sigma'] + c_7[\sigma]$	$c_9 = \frac{1}{56}$
odd * odd	
$\sigma' * \sigma' = [1] + c_8[\varepsilon'']$	
$\sigma' * \sigma = c_4[\varepsilon] + c_6[\varepsilon']$	
$\sigma * \sigma = [1] + c_5[\varepsilon] + c_7[\varepsilon'] + c_9[\varepsilon'']$	

TABLE 5
Fusion rules and structure constants for the fermion fields of the tricritical Ising model

$\psi * \psi = \bar{\psi} * \bar{\psi} = [1] + c_1[\varepsilon']$	
$\psi * \bar{\psi} = -\bar{\psi} * \psi = ic_1[\varepsilon] + ic_3[\varepsilon'']$	$c_1 = \frac{2}{3}\sqrt{\frac{\Gamma(\frac{4}{5})\Gamma^3(\frac{2}{5})}{\Gamma(\frac{1}{5})\Gamma^3(\frac{3}{5})}}$
$\psi * G = -\bar{G} * \bar{\psi} = ic_3[\varepsilon]$	$c_3 = \frac{3}{7}$

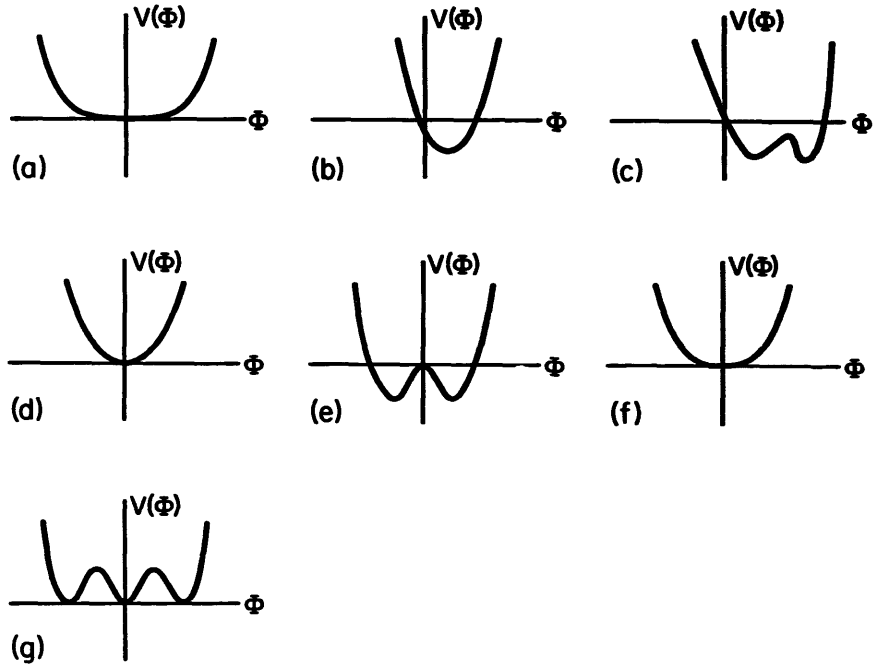

Fig. 1. Effective Landau–Ginzburg potentials for the Φ^6-theory: (a) at the tricritical point and perturbed by (b) the leading magnetic field, (c) the subleading magnetic field, the leading energy density with (d) $\lambda_2 > 0$ or (e) $\lambda_2 < 0$, the subleading energy density with (f) $\lambda_4 > 0$ or (g) $\lambda_4 < 0$.

by its relevant scaling fields in order of an increasing number of selection rules. The Landau–Ginzburg potentials for the perturbed theories are shown in fig. 1. Of course, the Landau–Ginzburg picture should not be taken literally since it does not properly take into account the anomalous dimensions of the fields, nor all the fusion rules of the two-dimensional theory.

4. Magnetic perturbations of the tricritical Ising model

Under the $\mathbb{Z}_2$ spin-reversal transformation, any magnetic operator ϕ changes sign: $Q^{-1}\phi Q = -\phi$. Hence the hamiltonians $H_{\pm\lambda} = H_0 \pm \lambda V$ are related by a

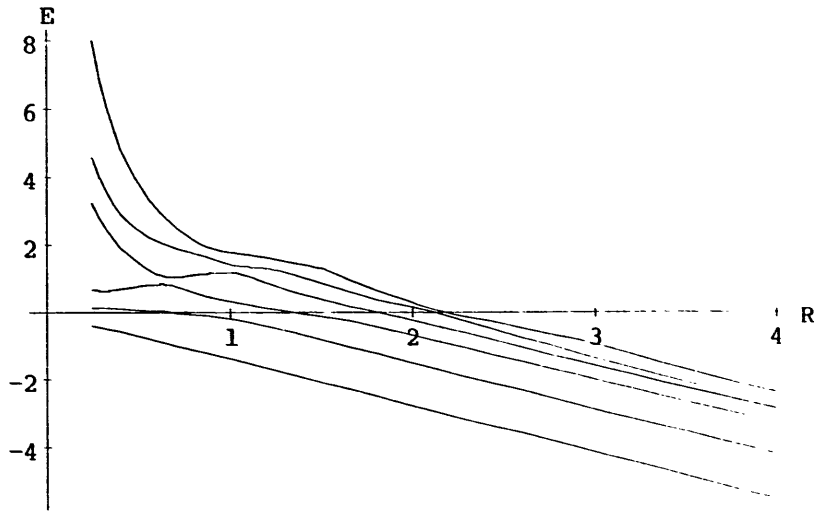

Fig. 2. Leading magnetic perturbation ($\lambda_1 = \pm 1$), $K = 0$ sector: the lowest six levels in the massive regime.

similarity transformation

$$H_{-\lambda} = Q^{-1} H_\lambda Q, \tag{4.1}$$

and the off-critical spectrum does not depend on the sign of the coupling constant λ.

4.1. LEADING MAGNETIC PERTURBATION

The field $\phi_{\frac{3}{80},\frac{3}{80}}$ is the most relevant scaling field of the tricritical Ising model, and it breaks all known symmetries of the critical theory. Fig. 2 shows the low-lying spectrum in the $K = 0$ sector as a function of the strip width R. We obtained these data from a truncated Hilbert space of 228 states, which includes all conformal states up to level 5 in the Verma modules. The lines show a clear massive infrared pattern as given by eq. (2.11). The effective scaling exponent

$$a = \frac{\mathrm{d} \ln E_0}{\mathrm{d} \ln R} \tag{4.2}$$

of the ground-state energy is shown in fig. 3 for a wider range of R. In this graph, one can distinguish the ultraviolet regime (2.9), the infrared regime (2.11), and the truncation-dominated regime (2.13).

The operator $\phi_{\frac{3}{80},\frac{3}{80}}$ is degenerate at level 4, and Zamolodchikov's counting argument [9] does not suggest that this deformation of the tricritical Ising model is integrable. We have checked explicitly that there are no conserved currents of spin 5 or spin 7. Of course, all this does not exclude the existence of conserved currents

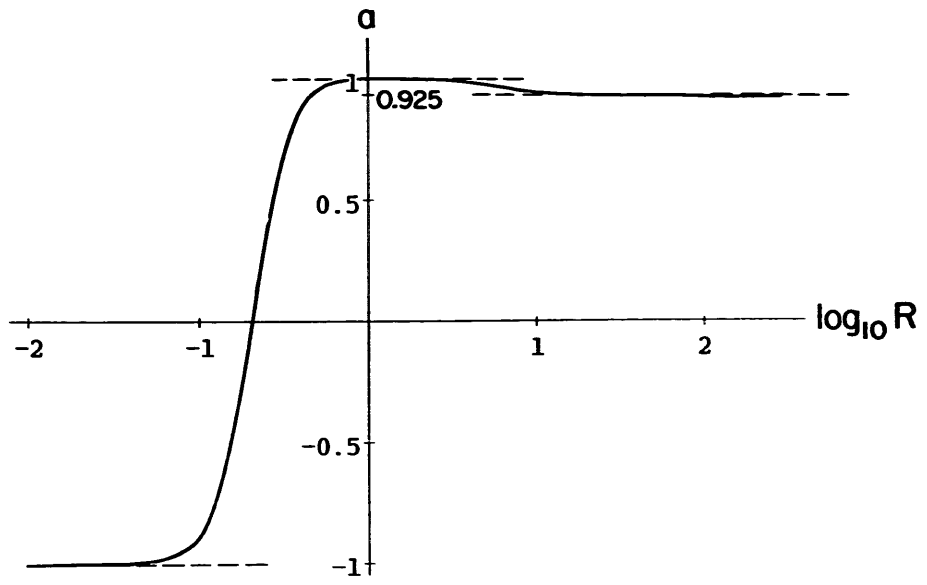

Fig. 3. Leading magnetic perturbation ($\lambda_1 = \pm 1$), $K = 0$ sector: the effective scaling exponent a of the ground-state energy, as defined in eq. (4.2).

with higher spin. But a plot of the crossover region (fig. 4) does not give any numerical evidence of integrability either; the lines repel each other.

In the infrared region, we extract the following masses below threshold (with a numerical accuracy of the order of one percent):

$$m_1, \qquad m_2 = 1.6(2)m_1, \qquad m_3 = 1.9(8)m_1. \tag{4.3}$$

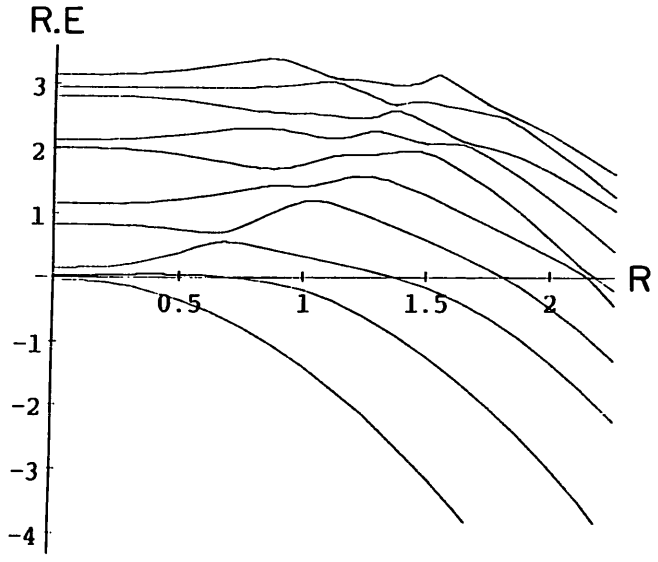

Fig. 4. Leading magnetic perturbation ($\lambda_1 = \pm 1$), $K = 0$ sector: the lowest ten levels in the crossover region.

TABLE 6
Mass spectrum of the E_8 Toda system

m_1	1
$m_2 = 2m_1 \cos(\pi/5)$	1.6180
$m_3 = 2m_1 \cos(\pi/30)$	1.9890
$m_4 = 4m_1 \cos(\pi/5)\cos(7\pi/30)$	2.4049
$m_5 = 4m_1 \cos(\pi/5)\cos(2\pi/15)$	2.9563
$m_6 = 4m_1 \cos(\pi/5)\cos(\pi/30)$	3.2183
$m_7 = 8m_1 \cos^2(\pi/5)\cos(7\pi/30)$	3.8911
$m_8 = 8m_1 \cos^2(\pi/5)\cos(2\pi/15)$	4.7834

These values are very close to those of the Ising model in a magnetic field at $T = T_c$ given in table 6 [9]. Henkel [25] recently found the same result using another numerical approach. It indicates that the effective dynamics of the two systems at length scales of the order of ξ are rather similar. However, we cannot conclude that the tricritical Ising model in a magnetic field is described by the same factorizable and elastic S-matrix as the Ising model in a magnetic field. The closure of the boot strap implies the existence of stable particles above threshold with fixed mass ratios m_i/m_1 [9,26,18], and this requires fine-tuning of the coupling constants to the integrable renormalization group trajectory. As shown in ref. [18], an arbitrarily small generic perturbation destroys the elasticity of the S-matrix: the particles above threshold decay into those below threshold (which cannot decay). Indeed, suppose that the hamiltonian (2.3) for $R \sim \xi$ is equivalent to the integrable hamiltonian of the Ising model in a magnetic field with a small amount of nonintegrability added. In the integrable system, the levels cross. The perturbation lifts the degeneracy at the crossing points and causes a splitting of the levels proportional to its matrix element between the two states. From fig. 2 we can read off the order of magnitude of such matrix elements to be $M \sim 10^{-1} m_1$. But the same perturbation also induces a shift of the (nondegenerate) levels E_i below threshold which is of the order

$$\Delta E_i \sim \sum_{j \neq i} M^2/(E_j - E_i) \sim 10^{-2} m_1 . \tag{4.4}$$

So it should not be surprising that the masses (4.3) are indistinguishable from those of the integrable system within our numerical accuracy.

4.2. SUBLEADING MAGNETIC PERTURBATION

The perturbation by $\phi_{\frac{7}{16},\frac{7}{16}}$ drives the tricritical Ising model into another massive regime (fig. 5). There is a single excitation m_1 below the threshold at about $2m_1$. The lowest two lines of the spectrum are interpreted as degenerate ground states.

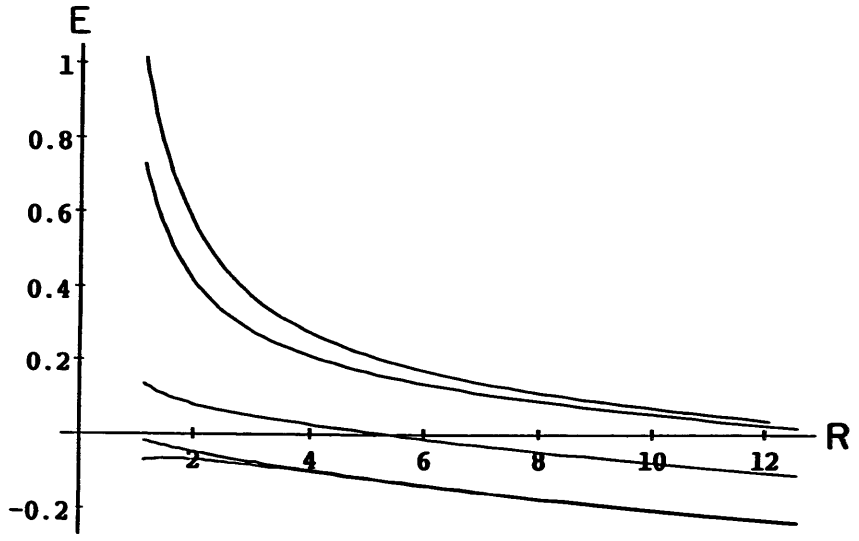

Fig. 5. Subleading magnetic perturbation ($\lambda_3 = \pm 0.1$), $K = 0$ sector: the lowest five levels in the massive regime.

In the crossover region, these two levels approach each other exponentially,

$$E_1 - E_0 \sim \mathrm{e}^{-R/\xi} \tag{4.5}$$

(see fig. 6 which should be compared with fig. 11). The scale ξ equals (up to a few percent within our accuracy) the inverse of the lowest mass m_1, as predicted in ref. [22]. In the usual three-dimensional phase diagram of the spin-1 Ising model in a magnetic field (see e.g. ref. [5]), there exist two "wings" of two-phase coexistence.

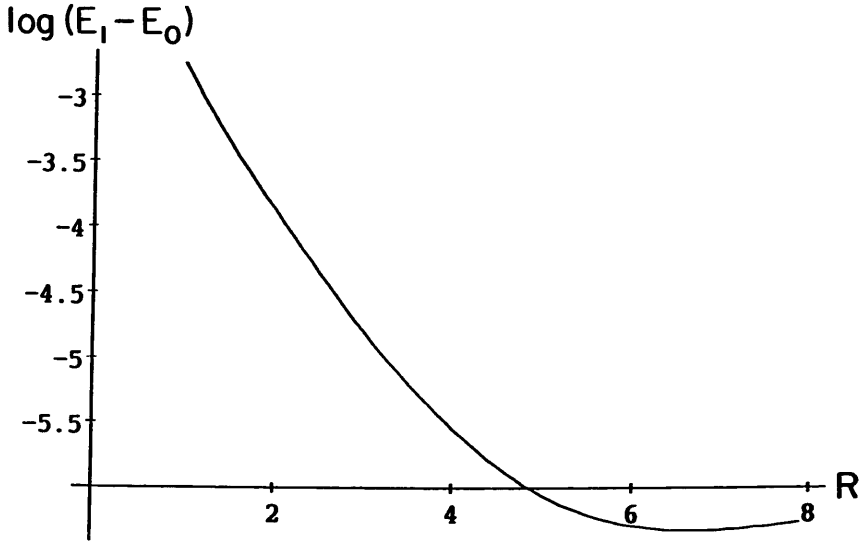

Fig. 6. Subleading magnetic perturbation ($\lambda_3 = \pm 0.1$), $K = 0$ sector: exponential splitting of the two lowest states in the crossover region, modified by truncation effects for $R \geqslant 3$.

At zero temperature, these phases correspond to the states $s = 0, 1$ or $s = 0, -1$, depending on the sign of the magnetic field. However, we should not identify the perturbation $\phi_{\frac{7}{16},\frac{7}{16}}$ as generating precisely these wings of phase coexistence. In fact, the thermodynamic state space of the theory (3.1) is four-dimensional. Hence its two-phase coexistence manifold is three-dimensional, and $\phi_{\frac{7}{16},\frac{7}{16}}$ generates a one-dimensional section of it.

One may speculate about the algebraic origin of the ground-state degeneracy. In the case of energy perturbations of the tricritical Ising model (which are discussed in sect. 5) or the Ising model, this degeneracy signals the spontaneous breakdown of the $\mathbb{Z}_2$ spin-reversal symmetry. The present case is more interesting, since the spin-reversal symmetry is explicitly broken. In the Landau–Ginzburg picture, this corresponds to the potential shown in fig. 1c. The field $\phi_{\frac{7}{16},\frac{7}{16}}$ is algebraically distinguished in another way: together with the identity and $\phi_{\frac{3}{2},\frac{3}{2}}$, it belongs to a subalgebra of the operator algebra (leading to a decomposition of the Hilbert space into two sectors which persists away from criticality), and it defines an integrable deformation of the tricritical Ising model. It is degenerate at level 2, and the counting argument shows that there are conserved currents with spins

$$s = 1, 5, 7, 11, 13. \tag{4.6}$$

In the crossover region, we observe crossing lines, even within a sector of the Hilbert space (see fig. 7). Furthermore, we checked that these crossings are specific to the integrable trajectory; the addition of a small $\phi_{\frac{3}{80},\frac{3}{80}}$-term removes all crossings.

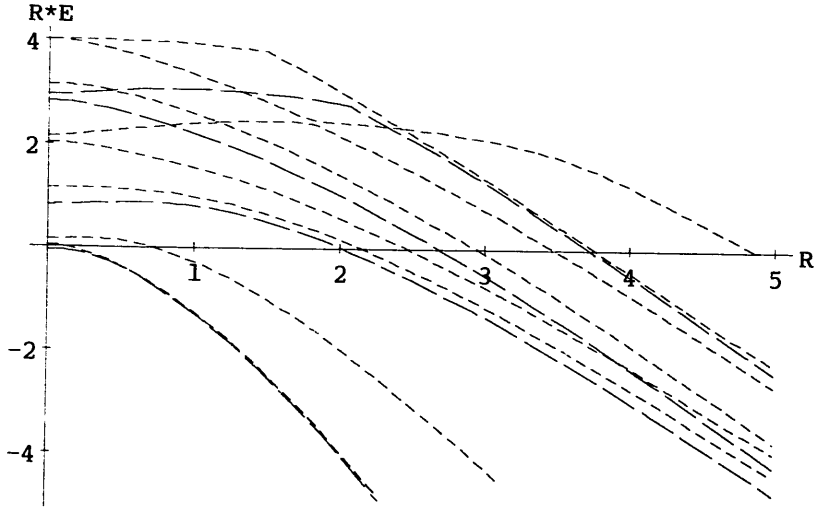

Fig. 7. Subleading magnetic perturbation ($\lambda_3 = \pm 0.1$), $K = 0$ sector: levels of the Hilbert space sector corresponding to the conformal subalgebra (long-dashed lines) and of the orthogonal sector (short-dashed lines) in the crossover region.

In the massive regime, the spectrum of excited states is quite different from that of the low-temperature Ising model, or the low-temperature tricritical Ising model. Since the ground state is degenerate, we expect to find a continuum of unbound kink–antikink pairs k_+, k_- with different relative momentum. In the finite-size system, the continuum will be replaced by a series of discrete lines approaching each other algebraically. We interpret the upper two states shown in fig. 5 as being part of this series. The isolated single line must therefore represent a bound state of a kink and an antikink. In the case of a spontaneously broken $\mathbb{Z}_2$ symmetry, one would expect two such degenerate bound states $|k_+k_-\rangle$ and $|k_-k_+\rangle$ (where the order indicates ordering on the line). However, in this case, there is no $\mathbb{Z}_2$ symmetry to enforce equality of the $k_+ - k_-$ and $k_- - k_+$ interactions. In the Landau–Ginzburg picture (fig. 1c), the potential well between the two vacua is indeed asymmetric. Thus it is possible that only one of the configurations k_+, k_- and k_-, k_+ can form a bound state, consistent with our findings. Interestingly enough, the mass of this bound state seems to be roughly degenerate with that of a single kink.

It would be interesting to consider this model further since it gives perhaps the simplest example of a system with two ground states that are not related by symmetry. Unfortunately, however, the perturbative approach is inflicted with difficulties. Using the methods of ref. [20,21], one can show that in an ε-expansion about $c = -2$ (where the perturbing field becomes marginal) at least the first three nontrivial terms of the β-function vanish.

5. Energy perturbations of the tricritical Ising model

These perturbations are even under spin reversal; the (off-critical) Hilbert space always decomposes into an even and an odd sector. Then it also makes sense to distinguish between periodic and $\mathbb{Z}_2$-twisted boundary conditions.

5.1. LEADING ENERGY PERTURBATION

5.1.1. Periodic boundary conditions. For $\lambda_2 > 0$, the perturbation $\phi_{\frac{1}{10},\frac{1}{10}}$ drives the system into the $\mathbb{Z}_2$-symmetric high-temperature phase. The massive theory is integrable and related to the Toda field theory based on the exceptional algebra e_7 [12,13,18]. The conserved currents have spin

$$s = 1,5,7,9,11,13,17 \qquad (\mathrm{mod}\, 18) \tag{5.1}$$

(these numbers are just the Coxeter exponents of e_7). The particle masses (table 7) and the S-matrix are known exactly [12,13]. The $\mathbb{Z}_2$ spin-reversal symmetry is manifest in the dynamics of the massive theory: the mass eigenstates can be classified into even and odd states (this corresponds to the $\mathbb{Z}_2$ symmetry of the

TABLE 7
The E_7 Toda system: mass spectrum and $\mathbb{Z}_2$ transformation of the states

m_1	1	odd
$m_2 = 2m_1 \cos(5\pi/18)$	1.2856	even
$m_3 = 2m_1 \cos(\pi/9)$	1.8794	odd
$m_4 = 2m_1 \cos(\pi/18)$	1.9696	even
$m_5 = 4m_1 \cos(\pi/18)\cos(\pi/9)$	2.5321	even
$m_6 = 4m_1 \cos(2\pi/9)\cos(\pi/9)$	2.8794	odd
$m_7 = 4m_1 \cos(\pi/18)\cos(\pi/9)$	3.7017	even

Dynkin diagram of the affine e_7), and the S-matrix in the disordered phase S_+ commutes with spin reversal Q,

$$S_+ = Q^{-1} S_+ Q. \tag{5.2}$$

The massive spectrum in the $K = 0$ sector is shown in fig. 8. The optimal point to read off the infrared spectrum (2.11) can be identified from fig. 9 which shows the effective scaling exponent (4.2) for the ground-state energy. Our numerical values for the masses below threshold,

$$m_1, \qquad m_2 = 1.2(8)m_1, \qquad m_3 = 1.8(7)m_1, \qquad m_4 = 1.9(6)m_1, \tag{5.3}$$

agree with the theoretical ones within our accuracy. Von Gehlen [23] obtained similar values from a finite-size analysis of the Blume–Capel model.

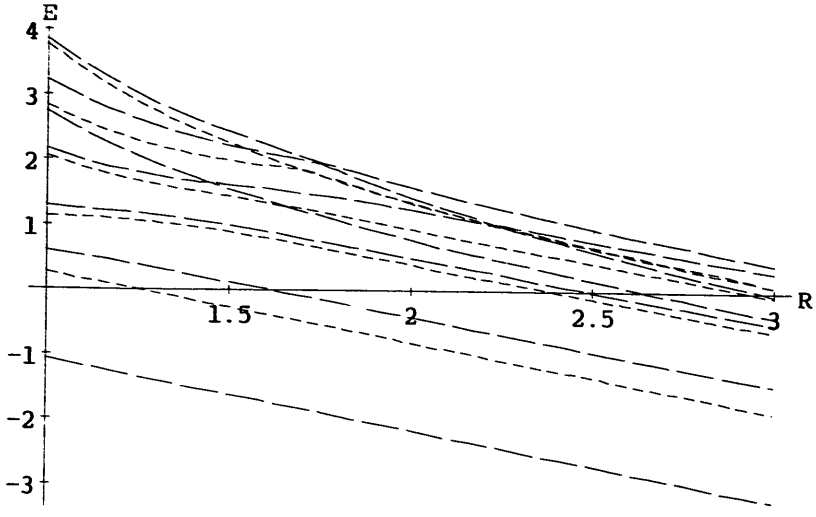

Fig. 8. Leading energy perturbation ($\lambda_2 = 1$), periodic boundary conditions, $K = 0$ sector: the lowest twelve lines in the massive regime. Long-dashed lines are even and short-dashed lines are odd under spin reversal. The short-dashed lines alone are the bosonic levels for twisted boundary conditions and $\lambda_2 = -1$.

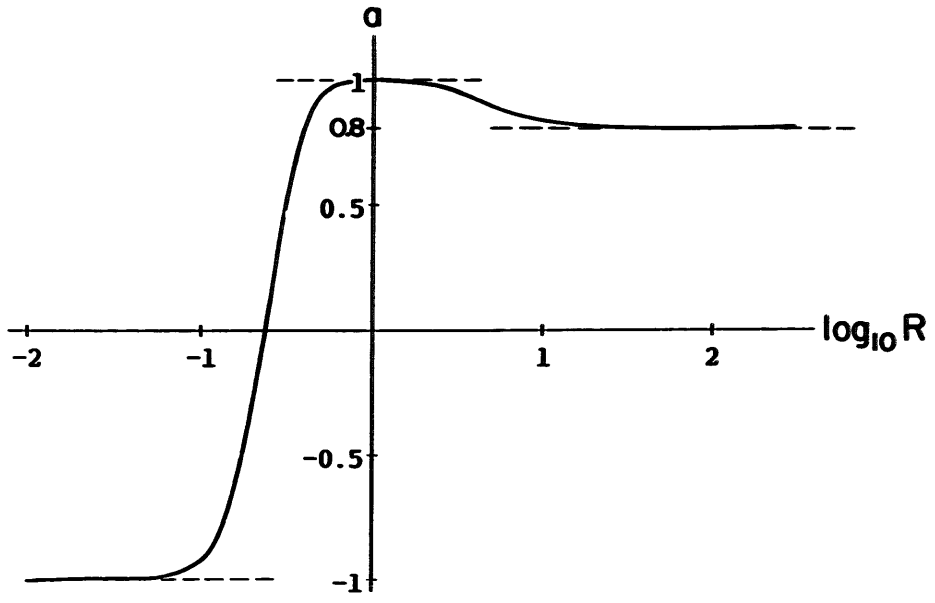

Fig. 9. Leading energy perturbation ($\lambda_2 = \pm 1$), periodic boundary conditions: effective scaling exponent a of the ground-state energy, as defined in eq. (4.2).

For $\lambda_2 < 0$, the situation is related by duality to the previous case. Since ε is odd under duality, we have

$$H_{-\lambda_2} = D^{-1} H_{\lambda_2} D. \tag{5.4}$$

The duality transformation maps the spin-even sector of the Hilbert space onto itself; therefore the even levels do not depend on the sign of λ_2. The odd states $|\sigma_i\rangle$ are mapped onto their duals $|\mu_i\rangle = D|\sigma_i\rangle$; the odd levels behave differently for $\lambda_2 < 0$. In the massive scaling region, they become degenerate with the even ones so that in the infrared theory (for periodic boundary conditions) only the levels

$$\varepsilon_0 R, \quad \varepsilon_0 R + m_2, \quad \varepsilon_0 R + m_4, \quad \varepsilon_0 R + 2m_1 \ \text{(threshold)}, \ldots \tag{5.5}$$

appear (the $K = 0$ sector is shown in fig. 10). The system is in a two-phase region of spontaneously broken spin reversal symmetry; in the thermodynamic limit there are two degenerate ground states

$$|+\rangle, \quad |-\rangle = Q|+\rangle. \tag{5.6}$$

In a finite volume, the two lowest states are split exponentially; fig. 11 shows this in the crossover region $R \sim \xi$. The massive excitations in the two-phase region are (anti)-kinks and bound states thereof. The conserved kink number (mod 2) now plays the role that the spin reversal symmetry had in the high-temperature phase.

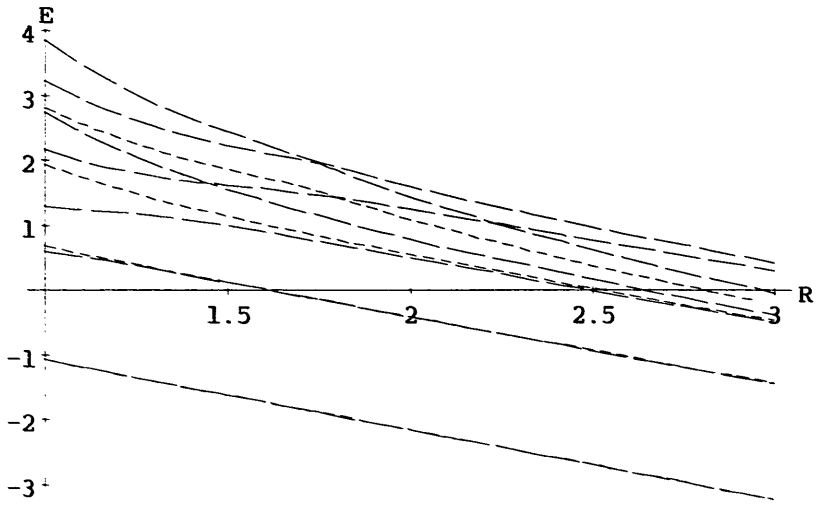

Fig. 10. Leading energy perturbation ($\lambda_2 = -1$), periodic boundary conditions, $K = 0$ sector: the lowest eleven levels in the massive two-phase region. Long-dashed lines are even and short-dashed lines are odd under spin reversal. The short-dashed lines alone are the bosonic levels for twisted boundary conditions and $\lambda_2 = 1$.

All mass eigenstates can be classified into even states (having an equal number of kinks and antikinks) and odd states (where those numbers differ by one). This is the unbroken $\mathbb{Z}_2$ symmetry $\tilde{Q}$ of the low-temperature phase which corresponds to the $\mathbb{Z}_2$ symmetry in the Dynkin diagram of the S-matrix in this phase S_-. It follows from eq. (5.4) that S_- is related to the S-matrix in the disordered phase S_+ by

$$S_- = D^{-1} S_+ D. \tag{5.7}$$

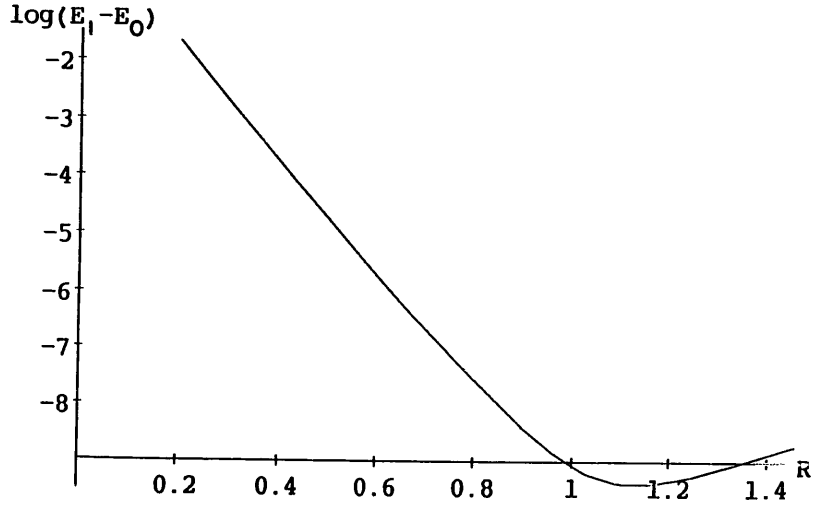

Fig. 11. Leading energy perturbation ($\lambda_2 = -1$), $K = 0$ sector: exponential splitting of the two lowest states in the crossover region.

Therefore the dynamics of the kinks and their bound states is described by the same elastic and factorizable S-matrix based on e_7. The spectrum consists of three odd particle masses m_1, m_3, m_6, and four even bound states with masses m_2, m_4, m_5 and m_7 (see table 7). The role of periodic boundary conditions is to restrict the *in*-states to the even sector. Since the kink number is conserved,

$$S_- = \tilde{Q}^{-1} S_- \tilde{Q}, \tag{5.8}$$

also the *out*-states are even. The $\mathbb{Z}_2$ symmetry ensures the equality of the $k_+ - k_-$ and $k_- - k_+$ interactions (unlike in the case of the subleading magnetic perturbation); so we expect, and indeed find, that all bound states are doubly degenerate.

5.1.2. Twisted boundary conditions. Twisted boundary conditions, on the other hand, restrict the bosonic Hilbert space to the disorder states $|\mu_i\rangle = D|\sigma_i\rangle$, which are odd under $\tilde{Q}$ and even under Q. By (5.4), the hamiltonian matrix elements between these states are given by those of the dual system:

$$\langle \mu_j | H_{-\lambda_2} | \mu_i \rangle = \langle \sigma_j | D^{-1} H_{-\lambda_2} D | \sigma_i \rangle = \langle \sigma_j | H_{\lambda_2} | \sigma_i \rangle . \tag{5.9}$$

Hence in the infrared theory for $\lambda_2 < 0$, only the states with an odd kink number appear (the short-dashed lines in fig. 8); the low-lying spectrum is

$$\varepsilon_0 R + m_1, \quad \varepsilon_0 R + m_3, \quad \varepsilon_0 R + m_1 + m_2 \ \text{(threshold)}, \ldots . \tag{5.10}$$

For $\lambda_2 > 0$, only the even levels (5.5) (the short-dashed lines in fig. 10) appear.

In addition to these bosonic levels, there are now states whose momenta are half-integer multiples of $2\pi/R$ (fermionic particles). They are odd under both Q and $\tilde{Q}$. Hence one expects (independently of the sign of λ) the infrared spectrum (5.10). This is confirmed by fig. 12, which shows the massive region of the $K = \pi/R$

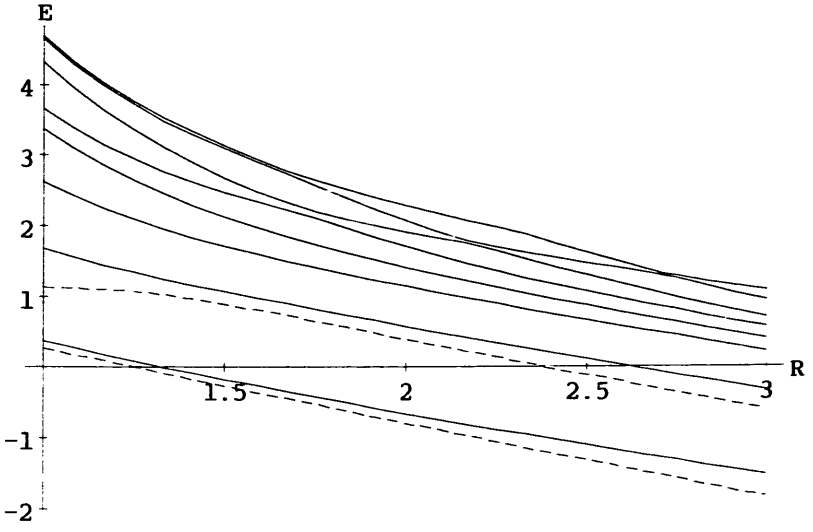

Fig. 12. Leading energy perturbation ($\lambda_2 = \pm 1$), twisted boundary conditions: the lowest eight levels of the sector $K = \pi/R$ (solid lines), together with the lowest two bosonic levels for $\lambda_2 = -1$ (short-dashed lines).

sector. The levels E_i^f in this sector show the following gaps*:

$$E_2^f - E_1^f \simeq 0.8(9)m_1, \qquad E_3^f - E_1^f \simeq 1.2(9)m_1, \ldots . \tag{5.11}$$

Thus for $T > T_c$, the combined infrared spectrum of bosons and fermions equals the spectrum (5.3) for periodic boundary conditions. This is necessary to ensure that correlation functions become independent of the boundary conditions in the thermodynamic limit. The quantum number Q classifying the levels can be reinterpreted as the fermion number (mod 2).

For $T < T_c$, the combined spectrum differs from the one in the periodic sector; only the masses (5.10) appear. The levels are pairwise exponentially split and become degenerate in the thermodynamic limit.

The S-matrix in the twisted sector should be related in a simple way to the S-matrix in the periodic sector.

5.2. SUBLEADING ENERGY PERTURBATION

The subleading energy operator ε' is even under spin reversal and duality. For $\lambda_4 > 0$, it is believed to induce the crossover to the critical Ising model [19]. The infrared behavior of the energy levels on the strip should be given by eq. (2.11),

$$\Delta E_i \simeq \frac{2\pi}{R} x_i, \tag{5.12}$$

where x_i are the scaling dimensions of the Ising model.

In its present form, however, the truncation method on the strip fails to reproduce this situation accurately. As fig. 13a shows for the ground state, the energy eigenvalues are strongly dependent on the level of truncation; for this perturbation, the Hilbert space truncated at level 5 is not yet a good approximation of the infinite-dimensional Hilbert space. But even in the absence of truncation effects, the asymptotic behavior (5.12) would be more difficult to extract since the corrections to it are also algebraically decaying and not exponentially as in the massive cases. However, our overall results are in no way consistent with a massive infrared theory. Fig. 13b shows, as an example, the lowest even excitation in the infrared region which is emerging at the highest level of truncation. In this region the pattern is consistent with the expected massless behavior of the Ising energy density, $\Delta E_2 \simeq 2\pi/R$.

* Measuring the lowest fermionic excitation $E_1^f - E_0$ involves the comparison of levels from different Hilbert space sectors. Since the truncation effects differ between sectors, this is considerably less accurate than measurements within one sector; we find $E_1^f - E_0 \simeq m_1$ only with an error of about ten percent (see the two lowest lines in fig. 12).

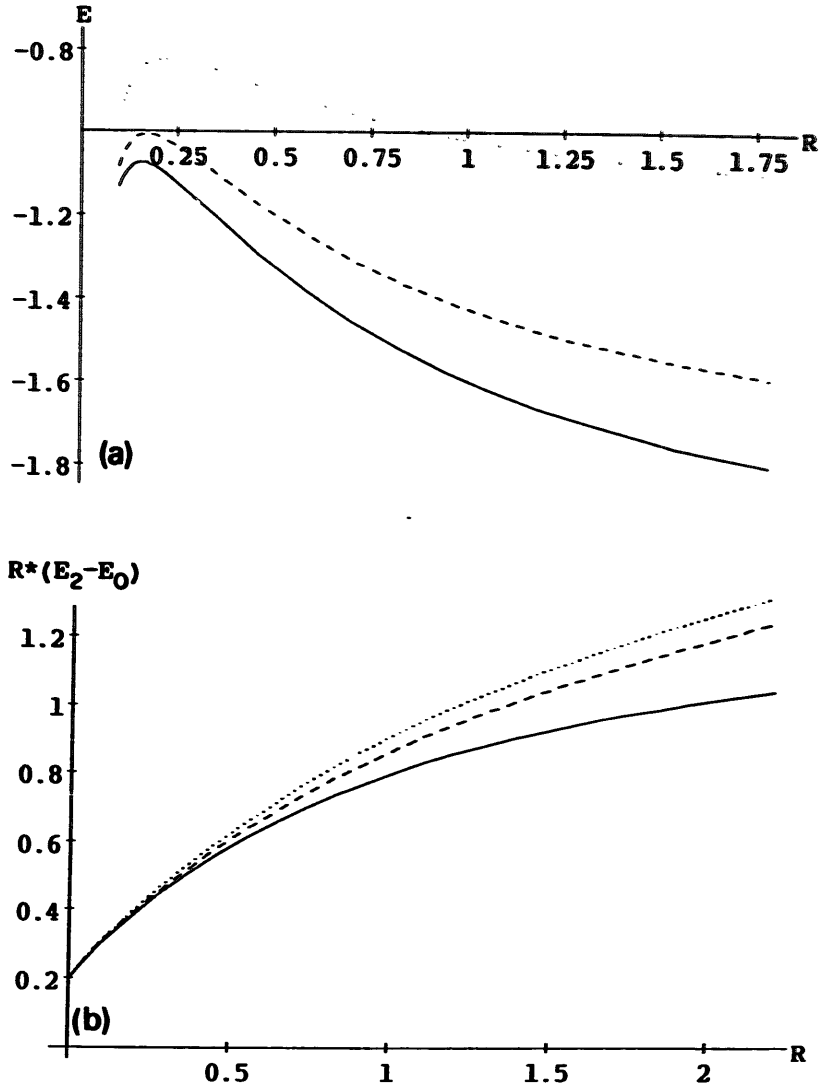

Fig. 13. Subleading energy perturbation ($\lambda_4 = 1$), periodic boundary conditions: truncation dependence of (a) the ground-state energy and (b) the lowest even excitation. Hilbert space truncation at level 3 (dotted), level 4 (dashed) and level 5 (solid).

For $\lambda_4 < 0$, the system is in the three-phase coexistence region [14]. The lowest three states are exponentially split in the finite-size system (fig. 15); in the thermodynamic limit there are three degenerate ground states

$$|0\rangle = Q|0\rangle = D|0\rangle, \qquad |+\rangle, \qquad |-\rangle = Q|+\rangle. \tag{5.13}$$

The massive theory is integrable. The lowest conserved charges with integer spin are easily identified by the counting argument; they are just the Coxeter exponents of su(2) [27]. It was conjectured by Zamolodchikov that the kinks do not form

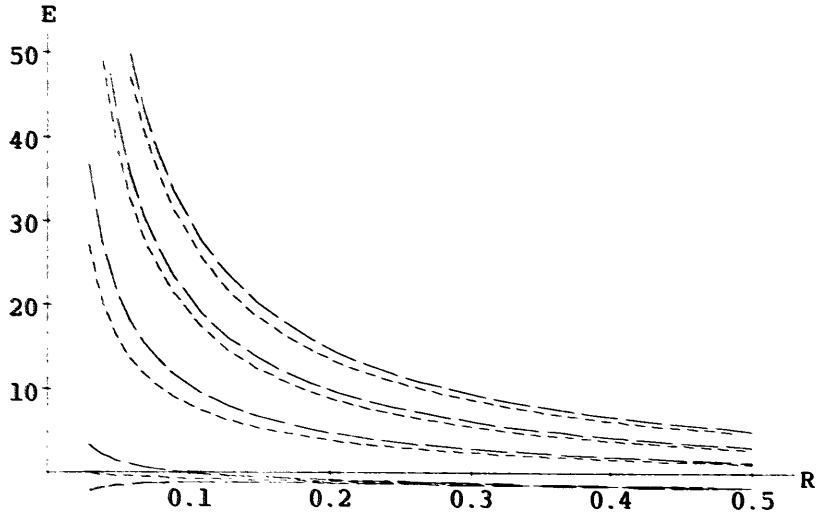

Fig. 14. Subleading energy perturbation ($\lambda_4 = -1$), periodic boundary conditions, $K = 0$ sector: the lowest nine levels in the massive three-phase coexistence region. Long-dashed lines are even and short-dashed lines are odd under spin reversal. The short-dashed lines alone are the bosonic levels for twisted boundary conditions and $\lambda_4 = -1$.

bound states [14]. This is confirmed by fig. 14 which shows that the lowest excitation is a doubly degenerate two-particle state (an unbound kink–antikink pair) at threshold.

Since

$$H_{\lambda_4} = D^{-1} H_{\lambda_4} D, \tag{5.14}$$

the bosonic levels in the twisted sector coincide with the odd levels in the periodic

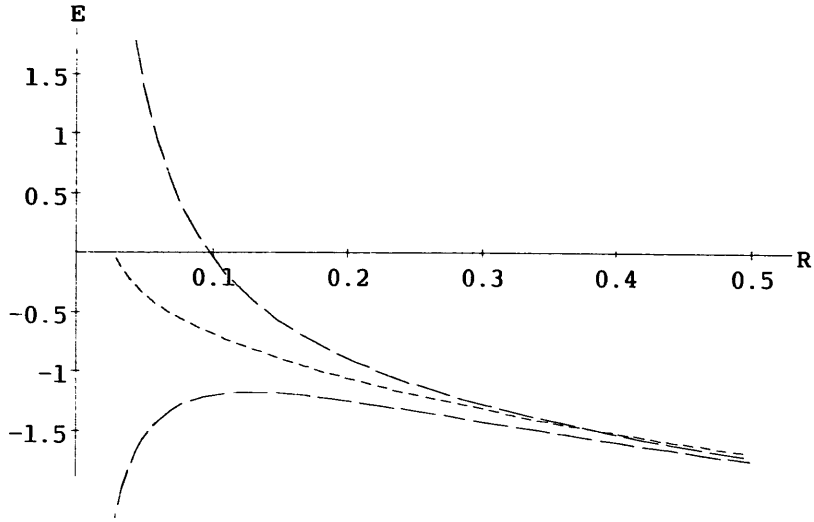

Fig. 15. Subleading energy perturbation ($\lambda_4 = -1$), periodic boundary conditions: exponential splitting of the three lowest states in the crossover region, modified by truncation effects for $R \geqslant 1$.

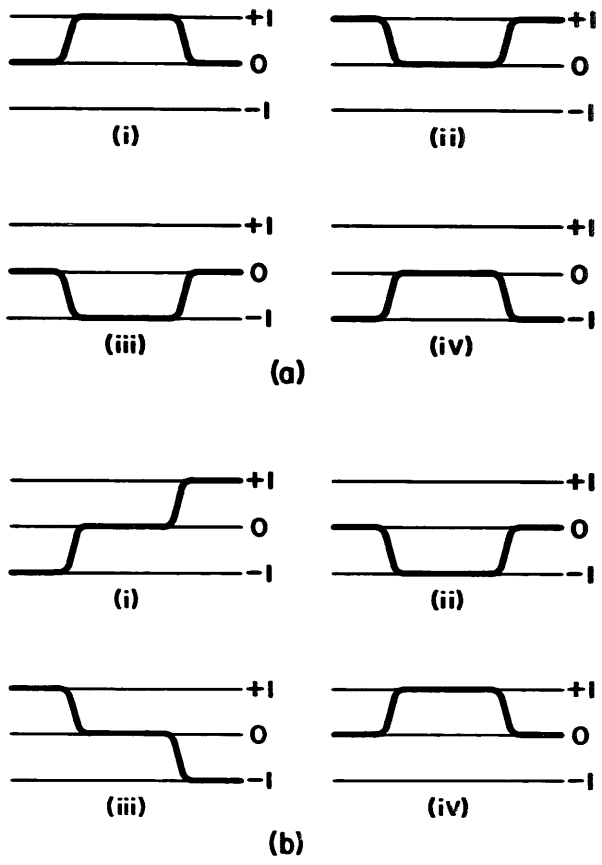

Fig. 16. Subleading energy perturbation ($\lambda_4 = -1$): unbound kink–antikink pairs in the three-phase coexistence region. (a) Periodic boundary conditions. The configurations (i) and (ii) represent the same $K = 0$ state, so do (iii) and (iv). (b) Twisted boundary conditions. All four configurations represent the same $K = 0$ state.

sector (the short-dashed lines in fig. 14). There is a nondegenerate ground state $|0\rangle$ (this state is unaffected by the twisting) and a single lowest two-particle excitation at threshold. One-kink states exist in neither case.

It is interesting to understand why the lowest state of the continuum is doubly degenerate with periodic boundary conditions, but non-degenerate in the twisted case. This may be seen in a semiclassical picture of the kinks. The kink–antikink pairs of the periodic sector are shown in fig. 16a. The lowest excitation is the $K = 0$ state, which is obtained by averaging over all positions of the kinks. Hence on a circle (i) and (ii) are in fact equivalent, so are (iii) and (iv). There are two independent states, related by spin reversal. In the finite volume, they are split exponentially. In the twisted sector, there are the four configurations of fig. 16b. When we join the ends of the line to form a Möbius strip, and average over all positions of the kinks to obtain the zero-momentum state, we find that all four configurations are equivalent. The reader is encouraged to make this experiment for him/herself.

6. Conclusions

In the following, we summarize our main results on the scaling region of the tricritical Ising model. The leading magnetic perturbation, generated by the field $\phi_{\frac{3}{80},\frac{3}{80}}$, breaks all known symmetries of the conformal theory. Accordingly, the spectrum of the off-critical hamiltonian shows no crossing lines. In the infrared theory, the masses below the threshold are very close to those of the Ising model in a magnetic field, indicating that the two systems have a similar dynamics at length scales of the order of the correlation length. Unlike the Ising model, however, the tricritical Ising model in a magnetic field is probably not integrable; hence the S-matrix is not purely elastic and there are no stable masses above threshold.

The subleading magnetic field, conjugate to $\phi_{\frac{7}{16},\frac{7}{16}}$, drives the system into a two-phase coexistence region. This fact may be related to the algebraic structure of the underlying ultraviolet field theory: $\phi_{\frac{7}{16},\frac{7}{16}}$ belongs to a subalgebra of the conformal algebra. This deformation of the tricritical Ising model is also integrable, and we see crossing lines in the spectrum that might signal the existence of additional conserved charges. There are massive kink states, and a single bound state whose mass appears to equal that of a single kink.

The leading energy perturbation $\phi_{\frac{1}{10},\frac{1}{10}}$ generates in the high-temperature phase the predicted spectrum of E_7. In the low-temperature phase, where the spin-reversal symmetry is spontaneously broken, only the odd or the even particles appear as kink states or bound states thereof, depending on the boundary conditions.

On the three-phase coexistence line, generated by the subleading energy operator $\phi_{\frac{6}{10},\frac{6}{10}}$ with a negative coupling constant, we observe the expected spectrum; the kinks do not form bound states in this case. The same perturbation with a positive coupling constant should induce the crossover to the Ising model. Our numerical data are consistent with this prediction, but they do not prove it, because they strongly depend on the level of truncation. Applying scaling theory to this dependence may be one way to improve the results in this case of a massless crossover.

We are grateful to Al.B. Zamolodchikov for his interest in our work and for several useful discussions. This work was supported in part by NSF Grant PHY 86-14185 and by INFN.

Appendix A

CONFORMAL HILBERT SPACE AND INTERACTION MATRIX ELEMENTS

The states of the conformal field theory organize into conformal families, i.e. products of holomorphic and antiholomorphic Verma modules (irreducible representations of the Virasoro algebra). Each Verma module $\mathscr{V}_\Delta$ contains one primary state $|\Delta\rangle$ of conformal dimension Δ and descendant states of dimension $\Delta + n$

TABLE A.1
The Verma modules of the tricritical Ising model: number $d(n, \Delta)$ of independent states (left column) and number $\hat{d}(n, \Delta)$ of quasi-primaries (right column)

n	$\Delta = 0$		$\Delta = \frac{3}{80}$		$\Delta = \frac{1}{10}$		$\Delta = \frac{7}{16}$		$\Delta = \frac{6}{10}$		$\Delta = \frac{3}{2}$	
0	1	1	1	1	1	1	1	1	1	1	1	1
1	0	0	1	0	1	0	1	0	1	0	1	0
2	1	1	2	1	1	0	1	0	2	1	2	1
3	1	0	3	1	2	1	2	1	2	0	2	0
4	2	1	4	1	3	1	3	1	4	2	3	1
5	2	0	6	2	4	1	4	1	5	1	4	1

$(n = 1, 2, \ldots)$. The number $d(n, \Delta)$ of linearly independent descendant states at level n is given by the character of the Verma module $\mathscr{V}_\Delta$,

$$\chi_\Delta(q) = q^{\Delta - c/24} \sum_{n=0}^{\infty} d(n, \Delta) q^n . \tag{A.1}$$

The Verma module can be decomposed into two orthogonal subspaces (this decomposition is convenient for the computation of the matrix elements below). The quasiprimary subspace consists of the states $|\delta\rangle$ which satisfy the equation $L_1|\delta\rangle = 0$ (and hence cannot be written as the derivative of states at the previous level). The number of linearly independent quasiprimary states at level n is $\hat{d}(n, \Delta) = d(n, \Delta) - d(n-1, \Delta)$. Table A.1 lists the values of $d(n, \Delta)$ and $\hat{d}(n, \Delta)$ $(n = 0, 1, \ldots, 5)$ for the six Verma modules of the tricritical Ising model. A basis in the quasiprimary subspace of $\mathscr{V}_\Delta$ may be obtained recursively as follows. At each level $n = 2, 3, \ldots$ there is one "primitive" quasiprimary state $P_n(\Delta)|\Delta\rangle$, where $P_1(\Delta)|\Delta\rangle = 1$ and $P_n(\Delta)$, $n \geqslant 2$, is a polynomial in the lowering operators L_{-k} given by

$$P_n(\Delta) = p_{n,n}(\Delta) L_{-n} + \sum_{l=1}^{n-1} p_{n,l}(\Delta) L_{-1}^{n-\hat{l}} P_l(\Delta) , \tag{A.2}$$

with $\hat{l} = 0$ if $l = 1$, $\hat{l} = l$ otherwise,

$$p_{n,l}(\Delta) = \begin{cases} 1 & \text{if } l = 1, \\ -\dfrac{2(2\Delta + 1)_{n-1}}{n+1} & \text{if } l = 2, 3, \ldots \text{ and } n = l, \\ -\dfrac{n!(2\Delta + l)_{n-l}}{l!(n-l)!(2\Delta + 2l)_{n-l}} & \text{if } l = 2, 3, \ldots \text{ and } n > l, \end{cases} \tag{A.3}$$

and $(a)_m = \Gamma(a + m)/\Gamma(a)$. The quasiprimary subspace of a nondegenerate Verma

module $\mathscr{V}_\Delta$ is spanned by the composite states

$$P_{n_k}(\Delta + n_{k-1} + \ldots + n_1) \ldots P_{n_2}(\Delta + n_1) P_{n_1}(\Delta)|\Delta\rangle, \tag{A.4}$$

with $n_k \leqslant n_{k-1} \leqslant \ldots \leqslant n_1$. In a degenerate Verma module, the null states have to be projected out. For the tricritical Ising model, we use the quasiprimary basis

$$|0\rangle, P_2(0)|0\rangle, P_2(2)P_2(0)|0\rangle,$$

$$|\tfrac{3}{80}\rangle, P_2(\tfrac{3}{80})|\tfrac{3}{80}\rangle, P_3(\tfrac{3}{80})|\tfrac{3}{80}\rangle, P_2(\tfrac{3}{80}+2)P_2(\tfrac{3}{80})|\tfrac{3}{80}\rangle, P_5(\tfrac{3}{80})|\tfrac{3}{80}\rangle, P_2(\tfrac{3}{80}+3)P_3(\tfrac{3}{80})|\tfrac{3}{80}\rangle,$$

$$|\tfrac{1}{10}\rangle, P_3(\tfrac{1}{10})|\tfrac{1}{10}\rangle, P_4(\tfrac{1}{10})|\tfrac{1}{10}\rangle, P_5(\tfrac{1}{10})|\tfrac{1}{10}\rangle,$$

$$|\tfrac{7}{16}\rangle, P_3(\tfrac{7}{16})|\tfrac{7}{16}\rangle, P_4(\tfrac{7}{16})|\tfrac{7}{16}\rangle, P_5(\tfrac{7}{16})|\tfrac{7}{16}\rangle,$$

$$|\tfrac{6}{10}\rangle, P_2(\tfrac{6}{10})|\tfrac{6}{10}\rangle, P_4(\tfrac{6}{10})|\tfrac{6}{10}\rangle, P_2(\tfrac{6}{10}+2)P_2(\tfrac{6}{10})|\tfrac{6}{10}\rangle, P_5(\tfrac{6}{10})|\tfrac{6}{10}\rangle,$$

$$|\tfrac{3}{2}\rangle, P_2(\tfrac{3}{2})|\tfrac{3}{2}\rangle, P_2(\tfrac{3}{2}+2)P_2(\tfrac{3}{2})|\tfrac{3}{2}\rangle, P_5(\tfrac{3}{2})|\tfrac{3}{2}\rangle, \tag{A.5}$$

which is truncated at level 5.

The orthogonal subspace consists of pure derivative states. Any such state at level n is of the form $L^r_{-1}|\delta\rangle$, where $|\delta\rangle$ is a quasiprimary state at level $n - r$. A holomorphic descendant state is thus characterized by three quantum numbers labelling its Verma module, its quasiprimary subfamily and its level.

The full Hilbert space is obtained by taking the tensor product of the holomorphic and antiholomorphic Verma modules for each conformal family. Each state is characterized by six quantum numbers. We truncate the Hilbert space at level 5, which leaves us e.g. for periodic boundary conditions with $\Sigma_{i=1}^{6}\Sigma_{n=0}^{5} d^2(n, \Delta_i) = 228$ states in the $K = 0$ sector.

The dimensionless interaction matrix elements between these states,

$$v_{ji}(\Delta, c) = \left(\frac{R}{2\pi}\right)^{2\Delta} \langle \phi_j | \phi_{\Delta,\Delta}(0,0) | \phi_i \rangle, \tag{A.6}$$

are analytic functions of the conformal dimensions Δ_i, Δ_j and Δ, and the central charge c. The matrix elements between primary states are fundamental structure constants which we extract from the crossing symmetric four-point functions in the plane [1, 6, 28]. The matrix elements between descendant states may then be obtained by repeated use of the relation

$$[L_m, \phi_{\Delta,\Delta}(\omega, \bar{\omega})] = z^m(m\Delta + z\partial/\partial z)\phi_{\Delta,\Delta}(\omega, \bar{\omega}) \tag{A.7}$$

and its complex conjugate. We compute first the matrix elements between the quasiprimary states (A.5) in a recursive way. The matrix elements between deriva-

tive states are then given by the formula [11]

$$\langle\delta|L_1^{r_2}\phi_\Delta(0)L_{-1}^{r_1}|\delta_1\rangle$$
$$= \langle\delta_2|\phi_\Delta(0)|\delta_1\rangle r_2! r_1!$$
$$\times \sum_{l=0}^{\min(r_1,r_2)} \frac{(\delta_2+\delta_1-\Delta)_l(\Delta+\delta_1-\delta_2)_{r_1-l}(\Delta+\delta_2-\delta_1)_{r_2-l}}{l!(r_1-l)!(r_2-l)!}. \tag{A.8}$$

The Hilbert space basis chosen is not orthonormal; the inner product between two states is

$$g_{ji}(c) \equiv \langle\phi_j|\phi_i\rangle = v_{ji}(0,c). \tag{A.9}$$

The interaction matrix elements appearing in the logarithm of the transfer matrix (2.3) are obtained from (A.6) by raising the index j,

$$v_i^{\mathrm{f}}(\Delta,c) = g^{\mathrm{f}j}(c)v_{ji}(\Delta,c). \tag{A.10}$$

We computed the matrix elements using a Mathematica computer program. The detailed algorithm is not specific to the tricritical Ising model; it will be published elsewhere [29].

References

[1] A.A. Belavin, A.M. Polyakov and A.B. Zamolodchikov, Nucl. Phys. B241 (1984) 333
[2] D. Friedan, Z. Qui and S. Shenker, Phys. Rev. Lett. 52 (1984) 1575
[3] A.B. Zamolodchikov, Sov. J. Nucl. Phys. 44 (1986) 529
[4] M. Blume, Phys. Rev. 141 (1966) 517;
H.W. Capel, Physica 32 (1966) 866;
R.B. Griffiths, Physica 33 (1967) 689;
M. Blume, V.J. Emery and R.B. Griffiths, Phys. Rev. A4 (1971) 1071;
M.J. Tejwani, O. Ferreira and O.E. Vilches, Phys. Rev. Lett. 44 (1980) 152
[5] I.D. Lawrie and S. Sarbach, *in* Phase transitions and critical phenomena, Vol. 9, ed. C. Domb and J. Lebowitz (Academic Press, New York, 1984)
[6] D. Friedan, Z. Qui and S. Shenker, Phys. Lett. B151 (1985) 37;
Z. Qiu, Nucl. Phys. B270 (1986) 235
[7] P. Goddard, A. Kent and D. Olive, Commun Math. Phys. 103 (1986) 105
[8] S. Lukyanov and V.A. Fateev, Lectures given in II Spring school on Contemporary problems in theoretical physics, Kiev 1988, preprints ITF-88-74-76P, Kiev 1988 (in Russian)
[9] A.B. Zamolodchikov, JETP Lett. 46 (1987) 160; Int. J. Mod. Phys. A3 (1988) 743; Integrable field theory from CFT, Proc. Taniguchi Symposium, Kyoto 1988, *in* Adv. Stud. Pure Math.
[10] A.B. Zamolodchikov, JETP Lett. 43 (1986) 730; Sov. J. Nucl. Phys. 46 (1987) 1090
[11] V.P. Yurov and Al.B. Zamolodchikov, Truncated conformal space approach to scaling Yang-Lee model, preprint ITEP 89-161
[12] P. Christe and G. Mussardo, Nucl. Phys. B330 (1990) 465
[13] V.A. Fateev and A.B. Zamolodchikov, Int. J. Mod. Phys. A5 (1990) 1025

[14] A.B. Zamolodchikov, Moscow preprint (October 1989)
[15] J.L. Cardy, Nucl. Phys. B270 [FS16] (1986); Nucl. Phys. B275 [FS17] 91986) 200; *in* Champs, cordes, et phénomènes critiques, Proc. 1988 Les Houches Summer School, ed. E. Brézin and J. Zinn-Justin (North-Holland, Amsterdam, 1989)
[16] Al. B. Zamolodchikov, Nucl. Phys. B 342 (1990) 695
[17] J.L. Cardy and G. Mussardo, Phys. Lett. B255 (1989) 275
[18] G. Mussardo and G. Sotkov, Bootstrap program and minimal integrable models, UCSBTH-89-64/ISAS-117-89
[19] D.A. Kastor, E.J. Martinec and S.H. Shenker, Nucl. Phys. B316 (1989) 590
[20] J.L. Cardy, J. Phys. A: Math. Gen. 20 (1987) L891
[21] M. Lässig, Nucl. Phys. B334 (1990) 652
[22] V. Privman and M.E. Fisher, Phys. Rev. B30 (1984), 322;
E. Brézin and J.Zinn-Justin, Nucl. Phys. B257 [FS14] (1985) 867
[23] G. von Gehlen, Nucl. Phys. B330 (1990) 741
[24] A. Cappelli, C. Itzykson and J.B. Zuber, Nucl. Phys. B280 [FS18] (1987) 445
[25] M. Henkel, The 2D tricritical Ising model in an external magnetic field, UGVA/DPT 1990/04-643
[26] P. Christe and G. Mussardo, Elastic S-matrices in $(1 + 1)$ dimensions and Toda field theories, UCSBTH-89-44
[27] T. Eguchi and S.K. Yang, Phys. Lett. B224 (1989) 373
[28] Vl.S. Dotsenko and V.A. Fateev, Nucl. Phys. B240 (1984) 312
[29] M. Lässig and G. Mussardo, Hilbert space and structure constants of descendant fields in two-dimensional conformal theories, UCSBTH-90-40